

# Closed-Loop Identification of Unstable Systems Using Noncausal FIR Models

Khaled Aljanaideh<sup>1</sup>, Benjamin J. Coffey<sup>1</sup>, and Dennis S. Bernstein<sup>2</sup>

**Abstract**—Motivated by the potential advantages of FIR model structures, the present paper considers the applicability of FIR models to closed-loop identification of open-loop-unstable plants. We show that FIR models can be used effectively for closed-loop identification of open-loop-unstable plants. The key insight in this regard is to realize that a noncausal FIR model can serve as a truncated Laurent expansion inside the annulus between the asymptotically stable pole of largest modulus and the unstable pole of smallest modulus. The key to identifying the noncausal plant model is to delay the measured output relative to the measured input. With this techniques, the identified FIR model is precisely a noncausal approximation of the unstable plant, that is, an approximation of the Laurent expansion of the plant inside the annulus of analyticity lying between the disk of stable poles and the punctured plane of unstable poles.

## I. INTRODUCTION

Identification of a plant during closed-loop operation is motivated by the need to monitor plant changes without opening the loop [1–3]. This need is unavoidable when the controlled plant is open-loop unstable, in which case opening the loop for system identification is prohibited. Even for plants that are open-loop asymptotically stable, opening the loop for system identification may not be feasible due to operational constraints. In these cases, system identification must rely on sensor-actuator data provided under operating conditions, although in some cases it may be possible to inject additional signals in order to enhance persistency and identifiability.

In addition to the fact that closed-loop identification constrains the choice of inputs, sensor and process noise inside the feedback loop lead to an errors-in-variables estimation problem with correlated noise. When the spectrum of this noise is known, consistency is achievable [4]. However, this information is usually not be available in practice, and decorrelation techniques are needed [5].

In the present paper we consider the problem of closed-loop identification of open-loop-unstable plants. Modified output error and Box-Jenkins models for unstable systems were derived in [6, 7]. Another approach to this problem is to assume a rational transfer function model whose coefficients are fit by least squares techniques. If the plant order is not known, then an overestimate of the order can be used, and the estimated model can be reduced to a more accurate order through approximation based on Markov parameters.

Approximation techniques are typically based on the Ho-Kalman realization theory [8] and its implementation in terms of the singular value decomposition [9]. This approach is highly sensitive to noise, however, although heuristics can be used to improve its accuracy [10–14].

An alternative approach to coefficient estimation is to use a  $\mu$ -Markov model structure, which is an overparameterized model that explicitly contains Markov parameters of the plant as a subset of the numerator coefficients [15, 16]. For the case of a white input signal and arbitrary, unknown output noise, standard least squares yields consistent estimates of the Markov parameters [17, 18]. The estimated Markov parameters can subsequently be used for approximation and order reduction.

The  $\mu$ -Markov model can be viewed as a hybrid model that possesses features of an FIR (finite-impulse-response) model. In particular, the numerator coefficients of an FIR model are precisely its Markov parameters, and all of its poles are located at zero. Although physical plants are rarely FIR, an FIR model can be considered as a candidate model structure for an asymptotically stable, IIR (infinite impulse response) plant. This approach is of interest since estimates of the numerator coefficients of an FIR model are expected to be more resistant to noise than the coefficients of an IIR model. An additional advantage of an FIR model structure is that Markov parameters are given explicitly by an FIR model but must be extracted from an IIR model.

Motivated by the potential advantages of FIR model structures, the present paper considers the applicability of FIR models to closed-loop identification of open-loop-unstable plants. At first glance this question seems questionable due to the fact that FIR models are highly asymptotically stable in the sense that all of their poles are located at zero. In the present paper we show that, in fact, FIR models can be used effectively for closed-loop identification of open-loop-unstable plants. The key insight in this regard is to realize that a noncausal FIR model can serve as a truncated Laurent expansion inside the annulus between the asymptotically stable pole of largest modulus and the unstable pole of smallest modulus.

The noncausal FIR model that approximates the Laurent expansion of an unstable plant involves both positive and negative powers of the Z-transform variable  $z$ . The negative powers approximate the stable part of the plant outside of a disk, whereas the positive powers approximate the unstable part of the plant inside a disk. Inside the common region of interest, which is the annulus in which the Laurent expansion converges, the identified model is noncausal, as evidenced by

<sup>1</sup> Graduate student, Department of Aerospace Engineering, The University of Michigan, Ann Arbor, MI 48109.

<sup>2</sup> Professor, Department of Aerospace Engineering, The University of Michigan, Ann Arbor, MI 48109.

the positive powers of  $z$ .

The key to identifying the noncausal plant model is to delay the measured output relative to the measured input. With this technique, the identified FIR model is precisely a noncausal approximation of the unstable plant, that is, an approximation of the Laurent expansion of the plant inside the annulus of analyticity lying between the disk of stable poles and the punctured plane of unstable poles.

The contents of the paper are as follows. In Section II we formulate the problem. In Section III we show the identification architecture. We show numerical examples in Section IV. In Section V we show how to reconstruct  $G$  from its noncausal FIR model. Finally, We give conclusions in Section VI.

## II. PROBLEM FORMULATION

Consider the closed-loop system in Figure 1 consisting of the SISO, discrete-time transfer function  $G$  of order  $n$  and the discrete-time controller  $C$ . We assume that the closed-loop system is internally asymptotically stable, although no assumptions are made on the stability of  $G$ . We assume that  $G$  has no poles on the unit circle.

Using partial fractions,  $G$  can be represented as

$$G(z) = G_s(z) + G_u(z) + D, \quad (1)$$

where  $D \triangleq G(\infty)$ , and  $G_s$  and  $G_u$  are the strictly proper asymptotically stable and strongly unstable parts of  $G$ , respectively. That is,  $G_u(z)$  is a transfer function all of whose poles are outside the closed unit disk.

The transfer function  $G$  is analytic in the annulus between the asymptotically stable pole of largest modulus and the unstable pole of smallest modulus with the Laurent expansion

$$G(z) = \sum_{i=-\infty}^{\infty} H_i z^{-i}, \quad (2)$$

$$H_i \triangleq \begin{cases} H_{u,i}, & \text{if } i < 0, \\ D, & \text{if } i = 0, \\ H_{s,i}, & \text{if } i > 0, \end{cases} \quad (3)$$

where for all  $i \geq 0$ ,  $H_{s,i}$  and  $H_{u,-i}$  are the coefficients of the Laurent expansions of  $G_s(z)$  and  $G_u(z)$ , respectively, in the given annulus.

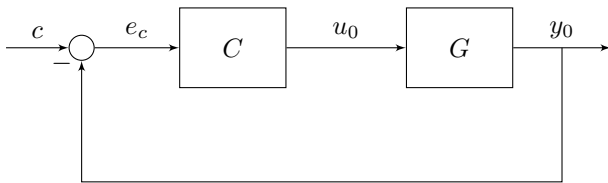


Fig. 1. Discrete-time closed-loop control system, where  $C$  is the controller, and  $G$  is the plant.  $G$  can be either an asymptotically stable or an unstable transfer function, and the closed-loop system is assumed to be internally stable.

Let  $d$  and  $r$  be positive integers, and define the FIR truncation of (2) by

$$G_{r,d}(z) \triangleq \sum_{i=-d}^r H_i z^{-i}. \quad (4)$$

Note that

$$G_{r,d}(z) \triangleq G_{s,r}(z) + G_{u,d}(z) + D, \quad (5)$$

where  $G_{s,r}(z)$  and  $G_{u,d}(z)$  are the causal and noncausal components of  $G_{r,d}(z)$ , respectively, defined by

$$G_{s,r}(z) \triangleq \sum_{i=0}^r H_{s,i} z^{-i}, \quad (6)$$

$$G_{u,d}(z) \triangleq \sum_{i=0}^d H_{u,-i} z^i. \quad (7)$$

Let  $p : \mathbb{C} \rightarrow \mathbb{C}$  be the polynomial

$$p(z) \triangleq \sum_{i=0}^n \alpha_i z^i, \quad (8)$$

where  $z \in \mathbb{C}$ , and  $\alpha_i \in \mathbb{R}$  for all  $i \in \{0, \dots, n\}$ . The flip  $F(p)$  of  $p$  is the polynomial

$$F(p(z)) \triangleq \sum_{i=0}^n \alpha_i z^{n-i}. \quad (9)$$

Since

$$F(p(z)) \triangleq \sum_{i=0}^n \alpha_{n-i} z^i, \quad (10)$$

the flip operator reflects the coefficients of the polynomial (8) from left to right.

Note that

$$\begin{aligned} G_{u,d}(z) &= \sum_{i=0}^d H_{u,-i} z^i = F \left( \sum_{i=0}^d H_{u,-i} z^{d-i} \right) \\ &= z^d F \left( \sum_{i=0}^d H_{u,-i} z^{-i} \right) = z^d F(G_{u,d}(z^{-1})). \end{aligned} \quad (11)$$

Hence (5) can be written as

$$G_{r,d}(z) = G_{s,r}(z) + z^d F(G_{u,d}(z^{-1})) + D. \quad (12)$$

## III. LEAST SQUARES IDENTIFICATION

In this section we use least squares with an FIR model structure to identify the transfer function  $G$  shown in Figure 1. We choose  $c$  to be a realization of a stationary white random process  $\mathcal{C}$ . Replacing  $z$  in (2) with the forward time-shift operator  $\mathbf{q}$  yields

$$G(\mathbf{q}) = \sum_{i=-\infty}^{\infty} H_i \mathbf{q}^{-i}. \quad (13)$$

It follows that

$$y_0(k) = \sum_{j=-\infty}^{\infty} H_j u_0(k-j), \quad (14)$$

which can be represented as

$$y_0(k) = \hat{y}_0(k) + e(k), \quad (15)$$

where the noncausal FIR model output  $\hat{y}_0(k)$  is defined as

$$\hat{y}_0(k) \triangleq \sum_{j=-d}^r H_j u_0(k-j), \quad (16)$$

and  $e(k)$  is the difference between the actual output and the noncausal FIR model output at time  $k$ . Note that, as  $d$  and  $r$  tend to infinity,  $e(k)$  tends to zero for all  $k \geq 0$ . Hence,  $d$  and  $r$  are chosen large enough such that  $e(k)$  is negligible for all  $k \geq 0$  and thus  $\hat{y}_0(k) \approx y_0(k)$ . Moreover, note from (16) that calculating the output at time  $k$  requires the inputs  $u_0(k-r), \dots, u_0(k+d)$ . That is, to identify a noncausal FIR model we first apply  $d$  time-delay steps to the measured output data and then perform identification between the input and the delayed output as we show next.

Consider the block diagram shown in Figure 2, where  $u_0$  is the input signal,  $y_0$  is the output signal, and  $v$  and  $w$  are input noise and output noise, respectively. We assume that  $v$  is zero-mean white noise that is independent of  $u$ , and  $w$  is zero-mean colored noise (i.e. not necessarily white) that is independent of  $u$ . Note that  $u$  and  $y$  represent measurements of the input  $u_0$  and the output  $y_0$ , respectively, such that

$$u = u_0 + v, \quad (17)$$

$$y = y_0 + w. \quad (18)$$

Note that (15) can be expressed as

$$y_0(k) = \theta_{r,d} \phi_{0,r,d}(k) + e(k), \quad (19)$$

where

$$\theta_{r,d} \triangleq \begin{bmatrix} H_{-d} & \cdots & H_r \end{bmatrix},$$

$$\phi_{0,r,d}(k) \triangleq \begin{bmatrix} u_0(k+d) & \cdots & u_0(k-r) \end{bmatrix}^T.$$

Moreover,

$$y(k) = \theta_{r,d} \phi_{r,d}(k) + e(k), \quad (20)$$

where

$$\phi_{r,d}(k) \triangleq \begin{bmatrix} u(k+d) & \cdots & u(k-r) \end{bmatrix}^T. \quad (21)$$

The least squares estimate  $\hat{\theta}_{r,d,\ell}$  of  $\theta_{r,d}$  is given by

$$\hat{\theta}_{r,d,\ell} = \arg \min_{\theta_{r,d}} \|\Psi_{y,\ell} - \bar{\theta}_{r,d} \Phi_{\mu,\ell}\|_F, \quad (22)$$

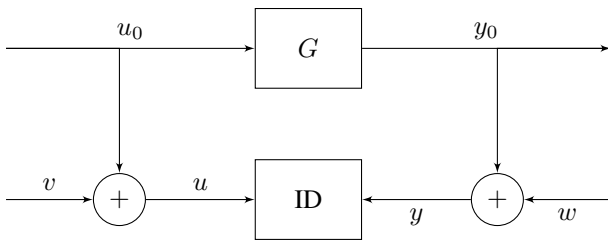


Fig. 2. Identification of the linear plant  $G$ .  $u_0$  and  $y_0$  represent input and output signals, respectively, where  $v$  and  $w$  represent input noise and output noise, respectively.

where  $\bar{\theta}_{r,d}$  is a variable of appropriate size,  $\|\cdot\|_F$  denotes the Frobenius norm,

$$\Psi_{y,\ell} \triangleq \begin{bmatrix} y(\mu) & \cdots & y(\ell-2d) \end{bmatrix},$$

$$\Phi_{\mu,\ell} \triangleq \begin{bmatrix} \phi_{r,d}(\mu+d) & \cdots & \phi_{r,d}(\ell-d) \end{bmatrix},$$

$\mu \triangleq r+d+1$ , and  $\ell$  is the number of samples.

#### IV. NUMERICAL EXAMPLES

We know from the previous sections that to identify the noncausal FIR model of a transfer function  $G$  we first apply  $d$  delay steps to the measured output data. Then we perform the identification process discussed in the previous section between the measured input data and the delayed output data. If a noncausal component of the identified FIR model appears, then  $G$  has at least one unstable pole; otherwise  $G$  is asymptotically stable.

In this section we show three examples. In each example,  $G$  is the plant in the closed-loop system shown in Figure 1. The input command  $c$  in Figure 1 is a realization of a stationary white random process  $\mathcal{C}$  with the gaussian pdf  $N(0,1)$ . Moreover, we assume that the intermediate signal  $u$  is accessible and persistently exciting. In this section we assume noise-free data, that is,  $v(k) = 0$  and  $w(k) = 0$  for all  $k \geq 0$ .

Define the prediction error (PE) as

$$\varepsilon \triangleq \|y - \hat{y}\|_2, \quad (23)$$

where  $y$  is the vector of the measured output and  $\hat{y}$  is the vector of the output of the FIR model structure as given by (16).

*Example 4.1:* Consider the unstable transfer function

$$G(z) = \frac{1}{z-1.5}, \quad (24)$$

and the PI controller

$$C(z) = 1.10 + 0.02 \frac{1}{z-1}. \quad (25)$$

Let  $r = 50$  and  $d = 50$ . Figure 3 shows the identified and actual impulse response of  $G$ . Note that the causal component of the impulse response is zero. Now we set  $r = 50$  and increase  $d$  from 0 to 50 output-delay steps to study the effect of delay on the prediction error. Figure 4 shows that the prediction error decreases as  $d$  increases since the identified FIR model using the delayed output captures a larger portion of the noncausal component of the Laurent expansion of  $G$ .

*Example 4.2:* Consider the unstable transfer function

$$G(z) = \frac{1}{(z-1.5)(z-0.5)}, \quad (26)$$

and the controller

$$C(z) = \frac{0.6z - 0.4103}{z - 0.3679}. \quad (27)$$

Let  $r = 50$  and  $d = 50$ . Figure 5 shows the identified and actual impulse response of  $G$ . Note that the impulse response

has both causal and noncausal components. Now we set  $r = 50$  and increase  $d$  from 0 to 50 output-delay steps to study the effect of delay on the prediction error. Figure 6 shows that the prediction error decreases as  $d$  increases since the identified FIR model using the delayed output captures a larger portion of the noncausal component of the Laurent expansion of  $G$ .

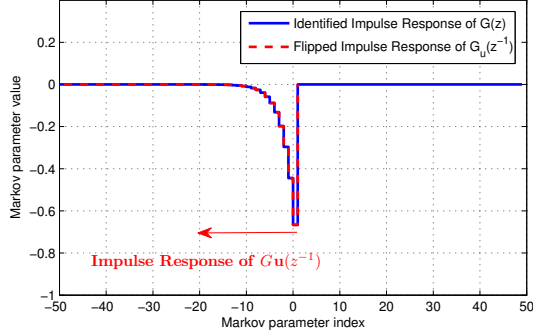


Fig. 3.  $G$  has one unstable pole as described in (24),  $r = 50$ , and  $d = 50$  output-delay steps. Note that the impulse response of  $G$  has only a noncausal component.

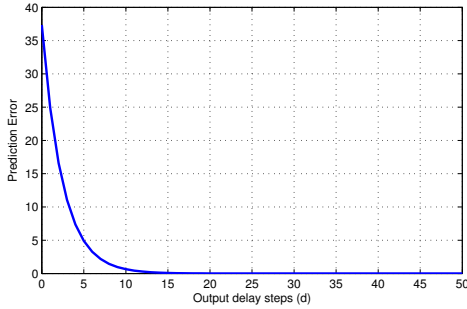


Fig. 4.  $G(z) = \frac{-1}{z-1.5}$  has one unstable pole,  $r = 50$ , and  $d$  increases from 0 to 50 output-delay steps. Note that the prediction error decreases as  $d$  increases since the identified FIR model using the delayed output captures a larger portion of the noncausal component of the Laurent expansion of  $G$ .

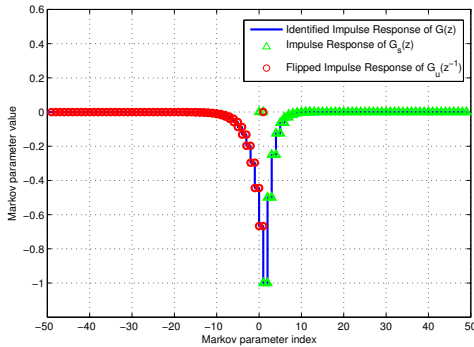


Fig. 5.  $G(z) = \frac{1}{(z-1.5)(z-0.5)}$  has one asymptotically stable pole and one unstable stable pole,  $r = 50$ , and  $d = 50$  output-delay steps. Note that the impulse response of  $G$  has both causal and noncausal components.

## V. RECONSTRUCTING $G$ FROM ITS NONCAUSAL FIR MODEL

In order to reconstruct  $G$  from its noncausal FIR model we reconstruct the stable and unstable parts of  $G$  separately using the eigensystem realization algorithm (ERA) [9]. Then, we obtain  $G$  by adding these two terms together as given in (1). Singular values of the Hankel matrix can be used to estimate the model orders  $n_s$  of  $G_s$  and  $n_u$  of  $G_u$ . We begin with initial estimates  $\hat{n}_s \geq n_s$  and  $\hat{n}_u \geq n_u$ . For  $G_s$ , we set  $r = 2\hat{n}_s - 1$  and  $d = 0$  in (22) and we obtain the estimated Markov parameters of  $G_s$  from (22). On the other hand, for  $G_u$ , we set  $r = 0$  and  $d = 2\hat{n}_u - 1$  in (22) and we obtain the estimated Markov parameters of  $G_u(z^{-1})$  from (22). Then, we construct the Markov block-Hankel matrix

$$\mathcal{H}(H_s) \triangleq \begin{bmatrix} H_{s,1} & \cdots & H_{s,\hat{n}_s} \\ \vdots & \ddots & \vdots \\ H_{s,\hat{n}_s} & \cdots & H_{s,2\hat{n}_s-1} \end{bmatrix}, \quad (28)$$

where  $H_s$  is the vector of Markov parameters defined as

$$H_s \triangleq [ H_{s,0} \quad \cdots \quad H_{s,2\hat{n}_s-1} ], \quad (29)$$

and  $\mathcal{H}(\cdot)$  is a linear mapping that constructs a Markov block-Hankel matrix from the components of the vector  $H_s$  except for  $H_{s,0}$ . The rank of  $\mathcal{H}(H_s)$  is equal to the McMillan degree of  $G_s$ . Similarly, for  $G_u(z^{-1})$  we construct the Markov block-Hankel matrix

$$\mathcal{H}(H_u) \triangleq \begin{bmatrix} H_{u,-2\hat{n}_u+2} & \cdots & H_{u,-\hat{n}_u+1} \\ \vdots & \ddots & \vdots \\ H_{u,-\hat{n}_u+1} & \cdots & H_{u,0} \end{bmatrix}, \quad (30)$$

where  $H_u$  is the vector of Markov parameters defined as

$$H_u \triangleq [ H_{u,-2\hat{n}_u+1} \quad \cdots \quad H_{u,0} ]. \quad (31)$$

Note that  $\mathcal{H}(\cdot)$  constructs a Markov block-Hankel matrix from the components of the vector  $H_u$  except for  $H_{u,-2\hat{n}_u+1}$ . The rank of  $\mathcal{H}(H_u)$  is equal to the McMillan degree of  $G_u(z^{-1})$ .

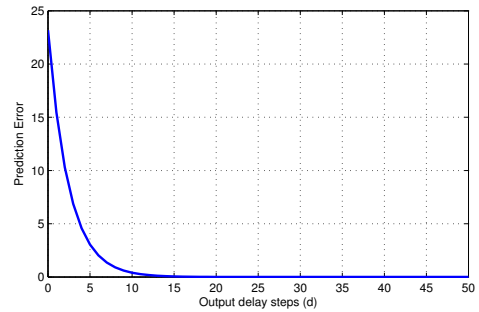


Fig. 6.  $G(z) = \frac{1}{(z-1.5)(z-0.5)}$  has one asymptotically stable pole and one unstable stable pole,  $r = 50$ , and  $d$  increases from 0 to 50 output-delay steps. Note that the prediction error decreases as  $d$  increases since the identified FIR model using the delayed output captures a larger portion of the noncausal component of the Laurent expansion of  $G$ .

We compute the singular values of  $\mathcal{H}(H_s)$  and  $\mathcal{H}(H_u)$  and look for a large decrease in the singular values. For noise-free data, a large decrease in the singular values is evident. Simulation results show that, even with a small amount of noise, the large decrease in the singular values disappears and thus the problem of estimating the model order becomes difficult.

The nuclear-norm minimization technique given in [10, 11] provides a heuristic optimization approach to this problem. In particular, define the optimization parameter vector  $\hat{H}_s$  as

$$\hat{H}_s \triangleq \begin{bmatrix} \hat{H}_{s,0} & \cdots & \hat{H}_{s,2\hat{n}-1} \end{bmatrix}. \quad (32)$$

To estimate the model order of  $G_s$  we solve the optimization problem

$$\text{minimize}_{\hat{H}_s} \left\| \mathcal{H}(\hat{H}_s) \right\|_N \quad (33)$$

$$\text{subject to} \left\| \hat{H}_s - H_s \right\|_F \leq \gamma_s, \quad (34)$$

where  $\|\cdot\|_N$  denotes the nuclear norm, and  $\gamma_s$  is varied from zero to  $\|\mathcal{H}(H_s)\|_F$ . For each value of  $\gamma_s$ , we find the optimal  $\hat{H}_s(\gamma_s)$ , and then we construct the Markov block-Hankel matrix  $\mathcal{H}(\hat{H}_s(\gamma_s))$  and compute its singular values. We define the  $\epsilon$ -rank of a matrix to be the number of nonzero singular values after setting all the singular values below  $\epsilon$  to zero. If, for a relatively wide range of  $\gamma_s$ , the same  $\epsilon$ -rank value is obtained, then we consider it to be the McMillan degree of  $G_s$ . Finally, we use ERA to construct the estimate  $\hat{G}_s$  of  $G_s$ .

Similarly, to estimate the model order of  $G_u(z^{-1})$  we solve the optimization problem

$$\text{minimize}_{\hat{H}_u} \left\| \mathcal{H}(\hat{H}_u) \right\|_N \quad (35)$$

$$\text{subject to} \left\| \hat{H}_u - H_u \right\|_F \leq \gamma_u, \quad (36)$$

where  $\gamma_u$  is varied from zero to  $\|\mathcal{H}(H_u)\|_F$ . For each value of  $\gamma_u$ , we find the optimal  $\hat{H}_u(\gamma_u)$ , and then we construct the Markov block-Hankel matrix  $\mathcal{H}(\hat{H}_u(\gamma_u))$  and compute its singular values. If, for a relatively wide range of  $\gamma_u$ , the same  $\epsilon$ -rank value is obtained, then we consider it to be the McMillan degree of  $G_u(z^{-1})$ . Finally, we use ERA to construct the estimate  $\hat{G}_u(z^{-1})$  of  $G_u(z^{-1})$ .

The following example illustrates this method.

*Example 5.1:* Consider the system (26). We use  $c$  in Figure 1 to be a realization of the stationary white random process  $\mathcal{C}$  with the gaussian pdf  $N(0, 1)$ . We add input and output noise with input signal-to-noise ratio of 100, and output signal-to-noise ratio of 10. We set  $r = 50$ ,  $d = 50$ , and  $\ell = 50,000$  points and then we identify the noncausal FIR model of  $G$ . Due to the input and output noise, we expect that the estimated Markov parameters to be within a small range of the actual Markov parameters. Figure 7 shows the Markov parameters of the noncausal FIR model of  $G$  for both cases with and without noise.

To choose the model order for  $G_s(z)$ , we set  $\hat{n}_s = 20$  and we solve the optimization problem (33), (34) for a range of

$\gamma_s$  from 0 to  $\|\mathcal{H}(H_s)\|_F$ . For each value of  $\gamma_s$ , we find the optimal  $\hat{H}_s(\gamma_s)$ , and then we construct the Markov block-Hankel matrix  $\mathcal{H}(\hat{H}_s(\gamma_s))$  and compute its singular values. We set  $\epsilon = 1 \times 10^{-5}$ , that is, all singular values below this threshold are set to zero, which yields the  $\epsilon$ -rank for each  $\gamma_s$ . Figure 8 shows a plot of  $\epsilon$ -rank( $\mathcal{H}(\hat{H}_s(\gamma_s))$ ) versus  $\gamma_s$ . We note that, for a relatively large range of  $\gamma_s$ , we have  $\epsilon$ -rank( $\mathcal{H}(\hat{H}_s(\gamma_s))$ ) = 2, which is close but not equal to the order of  $G_s$  (which is 1) due to noise. Using ERA we obtain

$$\hat{G}_s(z) = \frac{-0.9822z + 0.6657}{z^2 - 1.17z + 0.3364}. \quad (37)$$

Similarly, for  $G_u(z^{-1})$ , we set  $\hat{n}_u = 20$  and we solve the optimization problem (35), (36) for a range of  $\gamma_u$  from 0 to  $\|\mathcal{H}(H_u)\|_F$ . For each value of  $\gamma_u$ , we find the optimal  $\hat{H}_u(\gamma_u)$ , and then we construct the Markov block-Hankel matrix  $\mathcal{H}(\hat{H}_u(\gamma_u))$  and compute its singular values. We set  $\epsilon = 1 \times 10^{-5}$ , that is, all singular values below this threshold are set to zero, which yields the  $\epsilon$ -rank for each  $\gamma_u$ . Figure 9 shows a plot of  $\epsilon$ -rank( $\mathcal{H}(\hat{H}_u(\gamma_u))$ ) versus  $\gamma_u$ . We note that, for a relatively large range of  $\gamma_u$ , we have  $\epsilon$ -rank( $\mathcal{H}(\hat{H}_u(\gamma_u))$ ) = 1, which in fact is equal to the order of  $G_u(z^{-1})$ . Using ERA we obtain

$$\hat{G}_u(z^{-1}) = \frac{0.6486z}{-z + 0.6543}, \quad (38)$$

that is,

$$\hat{G}_u(z) = \frac{0.9913}{z - 1.5284}. \quad (39)$$

It follows that the estimate  $\hat{G}$  of  $G$  is

$$\begin{aligned} \hat{G}(z) &= \hat{G}_s(z) + \hat{G}_u(z) \\ &= \frac{0.0091z^2 + 1.007z - 0.684}{z^3 - 2.698z^2 + 2.12z - 0.5142}. \end{aligned} \quad (40)$$

Figure 10 shows bode plots for  $G$ ,  $\hat{G}$ , and  $\hat{G}_{r,d}$ . Note that the magnitude and phase plots of  $G(z)$ ,  $\hat{G}(z)$ , and  $\hat{G}_{r,d}(z)$  are close to each other.

## VI. CONCLUSIONS

In this paper we showed that FIR models can be used effectively for closed-loop identification of open-loop-unstable plants. To identify the noncausal plant model we delayed the measured output relative to the measured input, then we used least squares to estimate the causal and noncausal Markov parameters of the plant. Nuclear norm minimization was used to estimate the orders of the asymptotically stable and unstable parts of the plant. Finally, we reconstructed the plant from its stable and unstable parts using the eigensystem realization algorithm.

## REFERENCES

- [1] I. Gustavsson, L. Ljung, and T. Söderström, "Identification of processes in closed loop-identifiability and accuracy aspects," *Automatica*, vol. 13, pp. 59–75, 1977.
- [2] H. Hjalmarsson, M. Gevers, and F. de Bruyne, "For model-based control design, closed-loop identification gives better performance," *Automatica*, vol. 32, no. 12, 1977.
- [3] I. Landau, "Identification in closed-loop: a powerful design tool (better design models, simple controllers)," *Contr. Eng. Practice*, vol. 9, no. 1, p. 5165, 2001.

- [4] H. J. Palanthandalam-Madapusi, T. H. van Pelt, and D. S. Bernstein, "Parameter consistency and quadratically constrained errors-in-variables least-squares identification," *Int. J. Contr.*, vol. 83, no. 4, p. 862877, 2010.
- [5] M. Viberg, B. Wahlberg, and B. Ottersten, "Analysis of state space system identification methods based on instrumental variables and subspace fitting," *Automatica*, vol. 33, no. 9, pp. 1603–1616, 1997.
- [6] H. Hjalmarsson and U. Forsell, "Maximum likelihood estimation of models with unstable dynamics and non-minimum phase noise zeros," in *Proc. of 14th IFAC World Congress*, Beijing, China, 1999, pp. 13–18.
- [7] U. Forsell and L. Ljung, "Identification of unstable systems using output error and Box-Jenkins model structures," *Automatic Control, IEEE Transactions on*, vol. 45, no. 1, pp. 137–141, 2000.
- [8] B. Ho and R. Kalman, "Efficient construction of linear state variable models from input/output functions," *Regelungstechnik*, vol. 14, pp. 545–548, 1966.
- [9] J. N. Juang, *Applied System Identification*. Upper Saddle River, NJ: Prentice-Hall, 1993.
- [10] B. Recht, M. Fazel, and P. A. Parrilo, "Guaranteed minimum-rank solutions of linear matrix equations via nuclear norm minimization," *SIAM Review*, vol. 52, no. 3, pp. 471–501, 2010.
- [11] R. S. Smith, "Nuclear norm minimization methods for frequency domain subspace identification," in *Proc. Amer. Contr. Conf.*, Montreal, Canada, June 2012, pp. 2689–2694.
- [12] K. Usevich and I. Markovsky, "Structured low-rank approximation as a rational function minimization," in *Proc. SYSID*, Brussels, Belgium, July 2012, pp. 722–727.
- [13] I. Markovsky, "How effective is the nuclear norm heuristic in solving data approximation problems?" in *Proc. SYSID*, Brussels, Belgium, July 2012, pp. 316–321.
- [14] H. Hjalmarsson, J. S. Welsh, and C. R. Rojas, "Identification of box-jenkins models using structured arx models and nuclear norm relaxation," in *Proc. SYSID*, Brussels, Belgium, July 2012, pp. 322–327.
- [15] J. C. Akers and D. S. Bernstein, "Time domain identification using ARMARKOV / Toeplitz models," in *Proc. Amer. Contr. Conf.*, 1997, pp. 1667–1661.
- [16] T. H. Van Pelt and D. S. Bernstein, "Least squares identification using  $\mu$ -markov parameterizations," in *Proc. Conf. Dec. Contr.*, Tampa, FL, December 1998, pp. 618–619.
- [17] M. Kamrunnahar, B. Huang, and D. B. Fisher, "Estimation of markov parameters and time-delay/interactor matrix," *Chemical Engineering Science*, vol. 55, pp. 3353–3363, 1999.
- [18] M. S. Fledderjohn, M. S. Holzel, H. Palanthandalam-Madapusi, R. J. Fuentes, and D. S. Bernstein, "A comparison of least squares algorithms for estimating markov parameters," in *Proc. Amer. Contr. Conf.*, Baltimore, MD, June 2010, pp. 3735–3740.

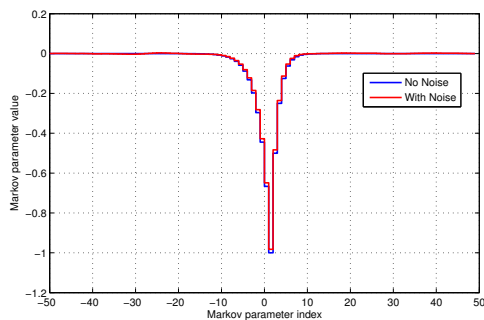


Fig. 7. Markov parameters of the noncausal FIR model of  $G(z) = \frac{1}{(z-1.5)(z-0.5)}$  with noise-free data (blue), and input and output noise with  $\text{SNR}_i = 100$  and  $\text{SNR}_o = 10$  (red).

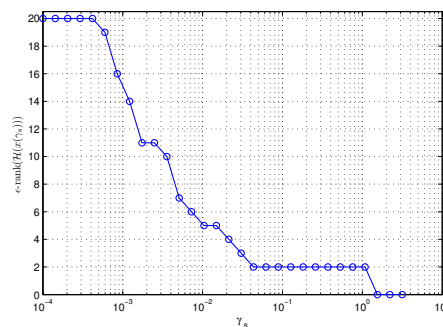


Fig. 8.  $\epsilon\text{-rank}(\mathcal{H}(\hat{H}_s(\gamma_s)))$  versus  $\gamma_s$ . Note that, for a relatively large range of  $\gamma_s$ , we have  $\epsilon\text{-rank}(\mathcal{H}(\hat{H}_s(\gamma_s))) = 2$ , which is close but not equal to the order of  $G_s$  (which is 1) due to noise.

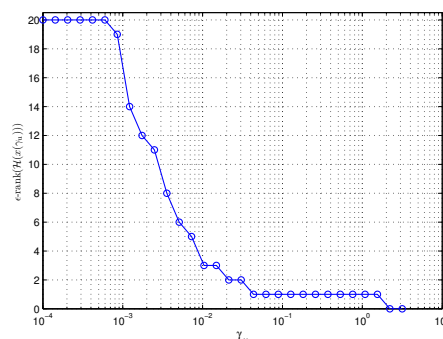


Fig. 9.  $\epsilon\text{-rank}(\mathcal{H}(\hat{H}_u(\gamma_u)))$  versus  $\gamma_u$ . Note that, for a relatively large range of  $\gamma_u$ , we have  $\epsilon\text{-rank}(\mathcal{H}(\hat{H}_u(\gamma_u))) = 1$ , which is equal to the order of  $G_u(z^{-1})$ .

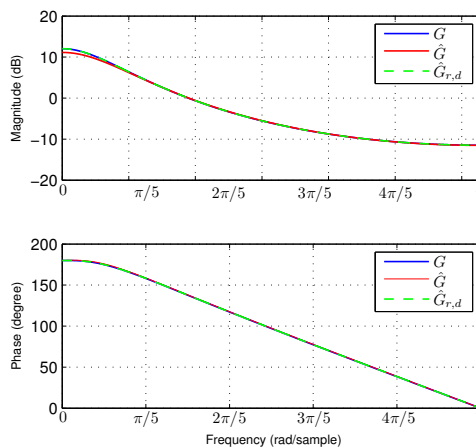


Fig. 10. Bode plots of  $G(z)$  (blue),  $\hat{G}(z)$  (red), and  $\hat{G}_{r,d}(z)$  (green). Note that the magnitude and phase plots of  $G(z)$ ,  $\hat{G}(z)$ , and  $\hat{G}_{r,d}(z)$  are close to each other.